Weierstraß-Institut
für Angewandte Analysis und Stochastik

Leibniz-Institut im Forschungsverbund Berlin e. V.

Preprint ISSN 2198-5855

Mapping atomic trapping in an optical superlattice onto the libration of a planar rotor in electric fields

Marjan Mirahmadi[1], Bretislav Friedrich[1], Burkhard Schmidt[2], Jesús Pérez-Ríos[1,3]

submitted: November 21, 2022

[1] Fritz-Haber-Institut der Max-Planck-Gesellschaft
Faradayweg 4-6
14195 Berlin, Germany
E-Mail: mirahmadi@fhi-berlin.mpg.de
bretislav.friedrich@fhi-berlin.mpg.de
jperezri@fhi-berlin.mpg.de

[2] Weierstrass Institute
Mohrenstr. 39
10117 Berlin, Germany
and
Institute for Mathematics
Freie Universität Berlin
Arnimallee 6
14195 Berlin, Germany
E-Mail: burkhard.schmidt@wias-berlin.de

[3] Department of Physics and Astronomy and
Institute for Advanced Computational Science
Stony Brook University
Stony Brook, NY 11794, USA
E-Mail: jesus.perezrios@stonybrook.edu

No. 2972
Berlin 2022

2020 *Mathematics Subject Classification.* 81Q05, 81Q60, 81Q80, 81V45, 81V55.

2010 *Physics and Astronomy Classification Scheme.* 33.15.Mt, 33.20.Xx, 37.10.Jk.

Key words and phrases. Atoms in optical lattices, super lattice, atom traps, molecules in external fields, combined fields, molecular quantum mechanics, Schrödinger equation, quasi-exact solvability, conditionally exact solvability.

We thank Tommaso Macrì (QuEra Computing, Cambridge, MA), Mikhail Lemeshko (Institute of Science and Technology Austria), and Dominik Schneble (Stony Brook University) and his group for helpful discussions. We also thank Konrad Schatz (Society for the Advancement of Applied Computer Science, Berlin) for his insightful comments. BF thanks John Doyle and Hossein Sadeghpour for their hospitality during his stay at Harvard Physics and at the Harvard & Smithsonian Institute for Theoretical Atomic, Molecular, and Optical Physics.

Edited by
Weierstraß-Institut für Angewandte Analysis und Stochastik (WIAS)
Leibniz-Institut im Forschungsverbund Berlin e. V.
Mohrenstraße 39
10117 Berlin
Germany

Fax: +49 30 20372-303
E-Mail: preprint@wias-berlin.de
World Wide Web: http://www.wias-berlin.de/

Mapping atomic trapping in an optical superlattice onto the libration of a planar rotor in electric fields

Marjan Mirahmadi, Bretislav Friedrich, Burkhard Schmidt, Jesús Pérez-Ríos

Abstract

We show that two seemingly unrelated problems – the trapping of an atom in a one-dimensional optical superlattice (OSL) formed by the interference of optical lattices whose spatial periods differ by a factor of two, and the libration of a polar polarizable planar rotor (PR) in combined electric and optical fields – have isomorphic Hamiltonians. Since the OSL gives rise to a periodic potential that acts on atomic translation via the AC Stark effect, it is possible to establish a map between the translations of atoms in this system and the rotations of the PR due to the coupling of the rotor's permanent and induced electric dipole moments with the external fields. The latter system belongs to the class of conditionally quasi-exactly solvable (C-QES) problems in quantum mechanics and shows intriguing spectral properties, such as avoided and genuine crossings, studied in details in our previous works [our works]. We make use of both the spectral characteristics and the quasi-exact solvability to treat ultracold atoms in an optical superlattice as a semifinite-gap system. The band structure of this system follows from the eigenenergies and their genuine and avoided crossings obtained as solutions of the Whittaker-Hill equation. Furthermore, the mapping makes it possible to establish correspondence between concepts developed for the two eigenproblems individually, such as localization on the one hand and orientation/alignment on the other. This correspondence may pave the way to unraveling the dynamics of the OSL system in analytic form.

1 Introduction

The spatial patterns imprinted upon ensembles of gaseous atoms by optical lattices have served as platforms for quantum simulation of condensed matter systems as well as for quantum information processing, including quantum computation [9, 29, 49, 36, 15, 13, 78, 12, 41, 28, 55, 40, 65]. Superimposed commensurate lattices (or superlattices for short) whose spatial periods are in integer ratios have enabled patterned loading key to achieving versatile atom-lattice architectures [51], quantum computing with atom transport [6], atom-pair manipulation [62], and topologically protected transport [43]. The engineering of optical lattices and superlattices has been recently reviewed in Ref. [76].

Herein, we show that the translational confinement of atoms in an optical superlattice (OSL) formed by the interference of optical lattices whose spatial periods differ by a factor of two can be mapped onto the libration of a planar rigid rotor (PR). This system is realized by subjecting a planar rotor to combined orienting and aligning interactions that arise due to the coupling of the rotor's permanent and induced dipole moments with collinear external electric fields [17, 18, 63, 16, 24, 5, 67, 64, 8, 30, 38, 53, 58, 32].

Interestingly, pulsed optical traps had been used earlier to simulate the kicked rotor [48, 1, 31] as a way of modelling quantum chaos and Anderson localization [14, 21, 26, 70, 22]. In contradistinction, our present study makes use of the previously established features of the driven rotor to shed light on the behavior of ultracold atoms confined in an optical superlattice. Among these features is the conditional quasi-exact solvability (C-QES) of the former system eigenproblem: under certain conditions (i.e., for particular ratios of the strengths of the orienting and aligning interactions), many (but not all) eigenfunctions and eigenenergies are available in analytic form. These can be then used, *inter alia*, to obtain the analytic form of several lattice band-edge states.

DOI 10.20347/WIAS.PREPRINT.2972 Berlin 2022

Moreover, the time-independent Schrödinger equation (TISE) of the planar rotor interacting with combined orienting and aligning fields is the Whittaker-Hill equation, i.e., a special case of the Hill differential equation [44]. This equation has very interesting spectral characteristics which leads to the semifinite-gap structure (every second gap is eventually closed) of the OSL system. To our knowledge, despite its intriguing spectral properties, the Wittaker-Hill equation has not been considered in the optical lattice literature. This is in contrast to the Mathieu equation (another special case of the Hill family) which is very well-known in the study of atoms in one-dimensional optical lattices consisting of single wells (only $\cos$ term). As a result we provide a new tool (perspective) to control the lattice configuration by using its depth and independent of the relative phase which has been subject of several previous works (see, e.g., Refs. [15, 6, 74, 43].

In addition, we have established a relationships between the main physical characteristics of the two eigenproblems such as localization on the one hand and directionality (orientation and alignment) on the other.

We note that also the Hamiltonian for molecular torsion in polyatomics [25], whether or not subject to coherent control [52, 50, 3], is isomorphic with the Hamiltonians of the two systems under consideration, see Fig. 1. However, in what follows we focus on the OSL and PR systems only.

This paper is organized as follows: In Sec. 2, we introduce the Hamiltonian of a single atom subject to an optical superlattice. The isomorphism of this Hamiltonian with that of the planar rotor in combined fields is established in Sec. 3. In Sec. 4, we provide a survey of the conditional quasi-exact solvability of the Schrödinger equation for either Hamiltonian. In Sec. 5, we make use of the spectral properties of the PR system to investigate the band structure of the atoms trapped in an optical superlattice. The spatial localization of the band-edge Bloch states and its relation to the orientation and alignment of the planar rotor is treated in Sec. 6. Finally, Sec. 7 provides a summary of the present work and outlines prospects for its future applications. A details the analytically obtainable band-edge states while B outlines the spectral properties of the Hill equation.

2 An atom interacting with a one-dimensional optical superlattice

A one-dimensional (1D) optical lattice, generated by the interference of two linearly polarized laser beams of the same wavelength λ counter-propagating along the x axis, produces, via the AC Stark effect, an optical trapping potential for atoms that is proportional to $\cos^2(kx)$, with $k = 2\pi/\lambda$ the wave-number of either of the laser beams. Superimposing two such optical lattices, characterized by wavevectors $k_i = 2\pi/\lambda_i$ with $i = 1, 2$, leads to a superlattice that produces an optical potential [51, 29, 6, 28]

$$V(x) = V_0 + V_1 \cos(2k_1 x) + V_2 \cos(2k_2 x - \varphi) \tag{1}$$

with $V_i = d^2\mathcal{E}_i^2/(2\hbar\Delta_i)$ the depth of the 1D lattice i, $\mathcal{E}_i$ the amplitude of the corresponding electric vector of the laser field, d the projection of the atomic dipole moment $\vec{d}$ on the electric field $\vec{\mathcal{E}_i}$ (note that d can be different for each lattice based on the atomic states involved), Δ_i the detuning of the laser field i from the nearest atomic resonance, and $\hbar$ the reduced Planck constant. The relative phase of the two superimposed lattices is characterized by the angle φ. The constant AC Stark shift V_0 between the two constituent lattices $i = 1$ and $i = 2$ will be omitted.

Provided the laser fields are sufficiently far detuned from any atomic resonance, i.e., $\Delta_i \gg \Gamma$, with Γ the spontaneous emission rate, we can invoke the adiabatic approximation [68] and write the effective

Hamiltonian for atoms in a 1D superlattice as[1]

$$H_{\mathrm{OSL}} = -\frac{\hbar^2}{2m}\frac{d^2}{dx^2} + V(x) \tag{2}$$

with m the atomic mass. Furthermore, as long as the scattering length of the atoms is small compared to the interatomic distance, we can treat the system as a non-interacting quantum gas.

In what follows, we consider a superlattice generated by the interference of two optical lattices whose spatial periods differ by a factor of two, i.e., $k_s \equiv k_1 = 2k_2$, where the subscript s labels the lattice with the shorter wavelength, λ_s. For now, we set the relative phase $\varphi = 0$. However, the effect of a non-zero relative phase on the properties of the superlattice and the solvability of the corresponding eigenvalue problem is the subject of our forthcoming work. Thus, Eq. 1 can be recast in the form

$$V(x) = V_s \cos^2(k_s x) + V_\ell \cos(k_s x) \tag{3}$$

which is suitable for establishing the mapping of the OSL onto the planar rigid rotor under the orienting ($\propto \cos$) and aligning ($\propto \cos^2$) interactions, i.e., onto the PR system. Note that in Eq. 3, we have neglected a constant shift of $V_s/2$ due to the transformation from $\cos$ to $\cos^2$. The amplitudes V_s ad V_ℓ, with the subscript ℓ pertaining to the lattice with the longer wavelength, λ_ℓ, are proportional to the depths of the “short” lattice, V_1, and “long” lattice, V_2, via

$$V_s = 2V_1 = \frac{\hbar\Omega_1^2}{4\Delta_1} \tag{4}$$

and

$$V_\ell = V_2 = \frac{\hbar\Omega_2^2}{8\Delta_2} \tag{5}$$

respectively, wherein $\Omega_i = -2\vec{d}\cdot\vec{\mathcal{E}}_i/\hbar$ is the Rabi frequency.

The optical potential 3 due to the superlattice is a periodic function with period (or “lattice constant”) $a = 2\pi/k_s$ whose shape depends on the relative magnitude and sign of the amplitudes V_ℓ and V_s. As shown in Fig. 2, for $V_s < 0$ the shape of the OSL potential can be varied from a single-well (SW) potential in the case $|V_\ell| > 2|V_s|$ to an asymmetric double-well (DW) potential when $|V_\ell| < 2|V_s|$ over the unit cell of the superlattice. For $|V_\ell| = 2|V_s|$, the potential has a flat maximum where the first, second, and third derivatives of the potential are zero. Hence the shape of the OSL potential for a given atom can be tailored by changing the ratio of the laser intensity to the detuning of the two constituent optical lattices.

The choice of the sign of V_ℓ is arbitrary since it is equivalent to a shift of $V(x)$ by half a period ($= \pi/k_s$) in x. Thus, without a loss of generality, we can assume $V_\ell > 0$, although the results and discussion presented below apply to both cases: for a blue-detuned ($\Delta_2 > 0$) as well as a red-detuned long lattice ($\Delta_2 < 0$). In contrast, the lattice geometry and its band structure are qualitatively different depending on whether V_s is positive or negative, as illustrated in Fig. 3. Hereafter, we consider the short lattice to have a red detuning, $\Delta_1 < 0$ (V_s negative), giving rise to an OSL potential consisting of an asymmetric double well with a local minimum, $(V_s + V_\ell)$, a global minimum, $(V_s - V_\ell)$, and a maximum, $-V_\ell^2/(4V_s)$, as shown in panel (a) of Fig. 3. Panel (b) shows what the OSL potential looks like for V_s positive.

[1] In this scenario, the atom can be treated as a two-level system whose evolution is described by that of its ground state.

Table 1: Correspondence between the interaction parameters of the OSL and PR eigenproblems.

System	Parameters			
Atom in an optical superlattice (OSL)	θ_a	V_s	V_ℓ	E_R
Planar rotor in external fields (PR)	θ	$-\zeta$	$-\eta$	B

3 Comparing an atom subject to an optical superlattice with a planar rotor subject to combined orienting and aligning interactions

The Hamiltonian of a planar (2D) rigid rotor subject to collinear orienting and aligning interactions is given by [57, 4, 46]

$$H_{\mathrm{PR}} = -B\frac{d^2}{d\theta^2} - \eta\cos\theta - \zeta\cos^2\theta \tag{6}$$

where $B = \hbar^2/(2I)$ is the rotational constant, with I the moment of inertia, and $0 \leq \theta < 2\pi$ is the polar angle between the axis of the rotor and the direction of the external collinear fields. It is the couplings of the permanent and induced dipole moments, fixed to the axis of the rotor, with the external collinear fields that give rise to the orienting and aligning interactions, see panel (b) of Fig. 1. The strengths of the orienting and aligning interactions are characterized, respectively, by the parameters η and ζ. For either a vanishing η or ζ, the time-independent Schrödinger equation (TISE) pertaining to the resulting Hamiltonian becomes isomorphic with the Mathieu equation, which satisfies different boundary conditions for the purely orienting and purely aligning interactions, cf. Table III of Ref. [18]. When both η and ζ vanish, the eigenproblem becomes that of a planar rotor.

In order to establish the isomorphism of Hamiltonians (2) and (6), we introduce a dimensionless variable $\theta_a \equiv k_s x$ ($= 2\pi x/a$) whose substitution transforms Hamiltonian (6) into

$$H_{\mathrm{OSL}} = -E_R\frac{d^2}{d\theta_a^2} + V_s\cos^2\theta_a + V_\ell\cos\theta_a \tag{7}$$

with $E_R = \hbar^2 k_s^2/(2m)$ the atomic recoil energy. Note that the recoil energy is related to the lattice constant a via $E_R = 2\pi^2\hbar^2/(ma^2)$. Comparing Hamiltonians 6 and 7 makes it possible to establish a correspondence between the interaction parameters of the OSL and PR eigenproblems, see Tab. 1.

Note that, unlike the polar angle θ, the variable θ_a in Eq. 7 is not defined on a circumference but on a line[1]. In particular, the interval $0 \leq \theta_a < 2\pi$ describes a unit cell consisting of an asymmetric double-well with a local minimum at $\theta_a = 0$ or 2π and a global minimum at $\theta_a = \pi$.

In order to explore the spectral properties of the two Hamiltonians given by Eq. 2 and 6, we divide the Schrödinger equation pertaining to each Hamiltonian through its characteristic energy, E_R or B. Thus, for the OSL system we obtain

$$\tilde{H}_{\mathrm{OSL}}\psi(\theta_a) = E\psi(\theta_a) \tag{8}$$

[1] In classical mechanics, the dynamics of a particle subject to a linear periodic potential is identical to that of a rotor, which is not the case for its quantum mechanical counterpart.

with $H_{\mathrm{OSL}}/E_R \to \tilde{H}_{\mathrm{OSL}}$. Hence the eigenvalues E of $\tilde{H}_{\mathrm{OSL}}$ pertaining to eigenfunctions $\psi(\theta_a)$ are rendered in units of recoil energy E_R.

On the other hand, the reduced eigenvalue problem for the PR system becomes

$$\tilde{H}_{\mathrm{PR}}\phi(\theta) = \epsilon\phi(\theta) \tag{9}$$

with $H_{\mathrm{PR}}/B \to \tilde{H}_{\mathrm{PR}}$. The eigenvalues ϵ of $\tilde{H}_{\mathrm{PR}}$ then come out in units of the rotational constant B. The corresponding eigenfunctions are $\phi(\theta)$.

Despite the above similarity of the OSL and PR eigenproblems, the physically meaningful boundary conditions on the two systems lead to different structures of the energy levels of Eqs. 8,9.

Due to its spatial periodicity, Eq. 8 can be treated via Floquet's theorem (or equivalently Bloch's theorem), with solutions obeying the boundary condition

$$\psi(\theta_a + 2\pi) = \mu\psi(\theta_a) \tag{10}$$

where $\mu = \exp(i2\pi q)$ is the Floquet multiplier and $2\pi\hbar q/a$ is the quasi-momentum. Consequently, the eigenvalues of Eq. 8 are energy bands $E \equiv E_n(q)$ with $n = 0, 1, 2, \cdots$ the band index. Note that the parameter q is continuous and confined to the first Brillouin zone (in the reduced-zone scheme), i.e., $-1/2 \leq q < 1/2$. For physically meaningful solutions, the modulus of μ must be equal to one, i.e., the parameter q must be real (see B).

In the case of the planar rotor interacting with combined fields, the TISE (9) may be solved either for a periodic boundary condition,

$$\phi(\theta + 2\pi) = \phi(\theta) \tag{11}$$

or an antiperiodic boundary condition[1],

$$\phi(\theta + 2\pi) = -\phi(\theta) \tag{12}$$

Given that Eqs. 11,12 are equivalent to Eq. 10 for $\mu = 1$ and $\mu = -1$, respectively, the (pendular) eigenstates of the planar rotor in combined fields correspond to Bloch waves for atoms in an optical superlattice with integer and half-integer wave numbers. In other words, the eigenfunctions and eigenvalues of the PR Hamiltonian are equivalent to those at the edges of the first Brillouin zone: the periodic solutions to $q = 0$ and the antiperiodic ones to $|q| = 1/2$.

4 Conditional quasi-exact solvability (C-QES) of the time-independent Schrödinger equation (TISE)

The solvability of the TISE (9) as well as its spectral properties have been studied by means of supersymmetry and Lie-algebraic methods in our previous work [57, 58, 4, 56, 46]. In this section, we make use of the results obtained therein to study the trapping of atoms in an optical superlattice. Based on the relation between Hamiltonians Eqs. 8,9, we provide analytic insights into the band-gap structure of the optical superlattice.

[1]We include these 2π-antiperiodic (or, equivalently, 4π-periodic solutions as they may prove useful for problems involving BerryâĂŹs geometric phase or systems with 4π rotational symmetry.

The TISE (9) for the PR system can be mapped onto the Whittaker-Hill differential equation [42, 75] (a special case of the Hill differential equation [44]),

$$\frac{d^2 f(y)}{dy^2} + \left[\lambda + 4\kappa\beta\cos(2y) + 2\beta^2\cos(4y)\right] f(y) = 0 \tag{13}$$

by making use of the definitions of the angular variable $y \equiv \theta/2$, the eigenvalues $\lambda \equiv (4\epsilon + 2\zeta)$, and the real parameters κ and β via

$$\eta/B = \kappa\beta \quad \zeta/B = \beta^2 \tag{14}$$

In the same way, we can map Eq. 8 for the OSL system onto the Whittaker-Hill differential equation by setting $y \equiv \theta_a/2$, $\lambda \equiv (4E - 2V_s)$, and

$$V_\ell/E_R = -\kappa\beta \quad V_s/E_R = -\beta^2 \tag{15}$$

The parameter κ has been termed the *topological index* [57, 58].

For $\zeta > 0$, the PR system belongs to the class of conditionally quasi-exactly solvable (C-QES) eigenproblems. This means that it is possible to obtain a finite number of its eigenvalues and eigenfunctions analytically (quasi-exact solvability, QES) [72, 71, 66, 19]), but only if the interaction parameters η and ζ satisfy a particular condition (conditional exact solvability, CES) [11, 27, 54]). Specifically, analytic solutions of Eq. 9 for the PR system only obtain for integer values of the topological index κ. In addition, the integer values of κ specify the number of obtainable analytic solutions.

Due to the PR $\mapsto$ OSL mapping, we see that the band-edge wavefunctions and energies of the optical superlattice with TISE (8) are analytically obtainable only for integer ratios

$$\kappa = \frac{|\eta|}{\sqrt{\zeta}} = \frac{|V_\ell|}{\sqrt{-V_s}} \tag{16}$$

Note that this statement is only valid for $V_s < 0$ as TISE (8) is not C-QES if the short-lattice is blue-detuned.

If κ is an odd integer, the first κ states obeying the periodic boundary condition (i.e., band-edge states with $q = 0$ or integer wavenumbers) are analytically obtainable. If κ is an even integer, the κ lowest antiperiodic solutions (i.e., band-edge states with $|q| = 1/2$ or half-integer wavenumbers) can be obtained analytically. In Refs. [4, 46], analytic expressions for forty PR eigenenergies $\epsilon(\beta)$ have been found. Those obtained for $\kappa = 1$ to $\kappa = 4$ are listed in Tab. 2 as band-edge energies $E(\beta) = \epsilon$. In addition, more details, including the analytic expressions for the band-edge eigenfunctions, are given in A.

We note that if $\beta \to 0$ as $\kappa \to \infty$ and, at the same time, $\kappa\beta$ remains finite, then the Whittaker-Hill equation (13) reduces to the Mathieu equation. As the above conditions of quasi-exact solvability do not apply to the Mathieu equation, it has no analytic solutions.

5 Atoms subject to an optical superlattice as a semifinite-gap system

The spectrum of a periodic Schrödinger operator consists of regions of allowed eigenvalues (bands) where the corresponding eigenfunctions are bounded, and forbidden eigenvalues (gaps), where the

Table 2: Analytically obtained lowest band-edge energies of the optical superlattice (eigenenergies $\epsilon^{(\Gamma)}$) for the first four values of κ defined in Eq. 16. Here Γ stands for the irreducible representations of the C_{2v} point group of H_{PR}.

κ	Γ	$E=\epsilon^{(\Gamma)}$
1	A_1	$-\beta^2$
2	B_1	$-\beta^2-\beta+1/4$
	B_2	$-\beta^2+\beta+1/4$
3	A_1	$-\beta^2-\frac{1}{2}\sqrt{16\beta^2+1}+1/2$
	A_1	$-\beta^2+\frac{1}{2}\sqrt{16\beta^2+1}+1/2$
	A_2	$-\beta^2+1$
4	B_1	$-\beta^2-\beta-\sqrt{4\beta^2+2\beta+1}+5/4$
	B_1	$-\beta^2-\beta+\sqrt{4\beta^2+2\beta+1}+5/4$
	B_2	$-\beta^2+\beta-\sqrt{4\beta^2-2\beta+1}+5/4$
	B_2	$-\beta^2+\beta+\sqrt{4\beta^2-2\beta+1}+5/4$

eigenfunctions do not have a finite norm and, therefore, are not physically meaningful. As shown in Sec. 3, for the TISE (8) of the OSL system, the bands only obtain for q real (in which case q corresponds to the Bloch wavenumber). The q parameter as a function of E can be determined from the Hill discriminant, $\mathcal{D}(E)$, by making use of the relation,

$$2\cos(2\pi q)=\mathcal{D}(E) \tag{17}$$

This procedure is commonly used to describe the band structure of a periodic differential equation such as the Hill equation [33, 34, 44, 69]. In B, we summarize the procedure resulting in Eq. 17, which is valid for any real and smooth periodic potential.

By making use of Eq. 17, it is straightforward to locate the allowed and forbidden energy regions: if q is real, $|\mathcal{D}(E)|\leq 2$, which defines the energy bands; if q is not real, $|\mathcal{D}(E)|>2$, which defines the energy gaps. In particular, the eigenvalues that satisfy $|\mathcal{D}(E)|=2$, define the band-edge states whose parameter q takes integer or half-integer values. In general, the Hill discriminant is an oscillating function of the (real) variable E that intersects the lines $\mathcal{D}(E)=\pm 2$ in the course of each oscillation. Consequently, the energy bands implied by the Hill equation obey the inequality $|\mathcal{D}(E)|\leq 2$. The bands are separated by forbidden regions (gaps) where $|\mathcal{D}(E)|>2$. However, for the TISE (8) of the OSL system, after a few oscillations, the Hill discriminant intersects only one of these two ± 2 lines and, eventually, touches but one of them without crossing it, as depicted in Fig. 4. A system with a spectrum whose every second gap is eventually closed is referred to as a *semifinite-gap system* [7, 23]. While the optical superlattice with potential $V(x)$ of Eq. 3 represents such a system, a system described by the Mathieu equation does not.

Since the eigenvalues E of the OSL system satisfying $\mathcal{D}(E)=\pm 2$ correspond to the spectrum of PR's TISE with periodic (+2) and antiperiodic (-2) boundary conditions, the knowledge of the PR spectrum provides a new perspective on the band structure of ultracold atoms in an optical superlattice, as encapsulated in Fig. 4.

As the symmetries of PR system are isomorphic with those of the C_{2v} point group [4], the solutions of the corresponding Schrödinger equation (9) fall into four categories, each corresponding to one of the irreducible representations $\Gamma\in\{A_1,A_2,B_1,B_2\}$ of C_{2v} [4, 46]. The solutions associated with the A_1 and A_2 symmetries are, respectively, even and odd functions (with respect to $\theta=\pi$), satisfying the periodic boundary condition on the interval $\theta\in[0,2\pi]$. The solutions corresponding to

B_1 and B_2 symmetries are, respectively, odd and even functions (with respect to $\theta = \pi$), satisfying the antiperiodic boundary condition[1]. In accordance with Sturm's oscillation theorem [44, 69], the eigenvalues form a monotonously increasing infinite sequence of real values $\epsilon_0^{(A)} < \epsilon_0^{(B)} \leq \epsilon_1^{(B)} < \epsilon_1^{(A)} \leq \epsilon_2^{(A)} < \epsilon_2^{(B)} \leq \epsilon_3^{(B)} < \ldots$, where $\{\epsilon_i^{(A)}\}$ is the energy set corresponding to the periodic solutions (either A_1 or A_2), and $\{\epsilon_i^{(B)}\}$ corresponds to the antiperiodic solutions (either B_1 or B_2). Furthermore, the number of nodes of the corresponding eigenfunctions in the interval $[0, 2\pi]$ is equal to $0, 1, 1, 2, 2, 3, 3, \ldots$, where the odd (even) number of nodes corresponds to antiperiodic (periodic) eigenfunctions.

Fig. 5 shows the energy levels of the planar rotor in combined fields as a function of the orienting parameter η for a constant value of the aligning parameter $\zeta = 50\,B$. The energy levels that lie beyond the C-QES interval, i.e., above the local minimum of the potential (marked by the upper dashed lines), have been obtained numerically by means of the Fourier grid Hamiltonian method [45] as implemented within the WavePacket software package [61, 59, 60]. For more details regarding the C-QES interval see A and Refs. [4, 46]. All eigenvalues below the local minimum of the potential, either analytic (integer κ) or numerical (non-integer κ), pertain to singlet states with a specific symmetry Γ. However, the energy differences between some pairs of the A and B levels in this part of the spectrum are small and hardly discernible on the scale of panel (a), which is why they are shown once more but separately: A levels in panel (b) and B levels in panel (c). Note that the ground state always pertains to the A_1 symmetry.

The most striking feature of the eigenenergies shown in Fig. 5 is their rich pattern of genuine and avoided crossings. As expected from the Wigner-von Neumann non-crossing rule [73, 35], levels pertaining to the same symmetry (i.e., to the same irreducible representations Γ) exhibit avoided crossings whereas levels of different symmetry exhibit genuine crossings.

For odd integer κ values, all eigenenergies corresponding to the periodic eigenstates A are two-fold degenerate, see panel (b) of Fig. 5. These degenerate states cannot be labeled by one of the specific symmetries, A_1 or A_2. Similarly, for even integer κ, the genuine crossings occur for the antiperiodic states B_1 and B_2, see panel (c) of Fig. 5. In other words, if κ is an odd (even) integer, the TISE (9) has two linearly independent solutions obeying the periodic (antiperiodic) boundary condition. This is referred to as coexistence of two linearly independent solutions with the same periodicity and is a peculiarity of the Whittaker-Hill equation (arising only for $\zeta > 0$) [10, 77, 44]. We note that the coexistence (degeneracy) of two Mathieu functions has been proved to be impossible [77].

On the other hand, the avoided crossings occur between pairs of states with the symmetry B_1 or B_2 (i.e., between the energy curves with the same colors in panel (c) of Fig. 5) for odd integer κ. For even integer κ, the avoided crossings occur between pairs of the A_1 or A_2 levels (i.e., between the energy curves with same colors in panel (b) of Fig. 5). Note that some of the avoided crossings cannot be discerned on the scale of the figure. Therefore, one may conclude that the energy curves show extrema at even κ. Although this is valid for the lower energy levels, it is not always true for higher energy levels and larger κ values.

The discussion above regarding the energy levels of the PR system can be extended to the case of ultracold atoms in an optical superlattice, completing the picture of its semifinite-gap structure. In particular, the energy bands ($|\mathcal{D}(E)| \leq 2$) of Eq. 8 are intervals

$$[\epsilon_0^{(A)}, \epsilon_0^{(B)}], \ [\epsilon_1^{(B)}, \epsilon_1^{(A)}], \ [\epsilon_2^{(A)}, \epsilon_2^{(B)}], \ \cdots \tag{18}$$

[1]Note that the correlation between the even functions and B_2 (or odd functions and B_1) is valid for $\eta < 0$ and will change to the correlation between even functions and B_1 (odd functions and B_2) for $\eta > 0$. For more details, see Refs. [4, 46]

separated by the gaps ($|\mathcal{D}(E) > 2$) whose edges correspond to the PR's eigenfunctions of the same periodicity: A-type gaps for periodic ($|q| = 0$) and B-type gaps for the antiperiodic ($|q| = 1/2$) boundary conditions, i.e.,

$$(\epsilon_0^{(B)}, \epsilon_1^{(B)}), \ (\epsilon_1^{(A)}, \epsilon_2^{(A)}), \ (\epsilon_2^{(B)}, \epsilon_3^{(B)}), \ \cdots \tag{19}$$

Therefore, the genuine crossings in PR's spectrum correspond to the closed gaps in the optical superlattice band structure. For even integer κ, all B-type gaps are closed except for the first $\kappa/2$. In addition, using the analytical energies (see Secs. 4,A), it is possible to derive analytic expressions for the widths of these $\kappa/2$ open B-type gaps. If κ is an odd integer, all A-type gaps vanish except for the first $(\kappa-1)/2$, whose widths can be calculated analytically. The semifinite-gap structure for two examples, $\kappa = 2$ and $\kappa = 3$, are shown, respectively, in panels (a) and (b) of Fig. 4.

The band structure of atoms in an optical superlattice for constant $V_s = -5\ E_R$ and different V_ℓ is shown in Fig. 6. Note that while the energy bands below the maximum of the potential (i.e., below the upper black dashed line) are hardly discernible, those sufficiently above the potential's maximum exhibit a significant width. However, the gaps shrink with the energy of the band. These differences are more prominent when the optical superlattice has deeper wells, as can be seen by comparing Fig. 5 with Fig. 6. Furthermore, guided by the color-coding assigned to different Γ symmetries, we can see that with every transition from a genuine crossing (i.e., V_ℓ corresponding to closed gaps), the symmetry of the lower and upper band-edge states involved is interchanged ($A_1 \leftrightarrow A_2$ or $B_1 \leftrightarrow B_2$). We note that even though the gaps decrease in the high energy limit, the gaps become zero only at the loci of integer κ. Although further into the single-well regime (on the right from the red dotted vertical line in Fig. 6) the avoided and genuine crossings in principle still occur, the characteristic features of the double-well regime fade out, see Fig. 6.

Fig. 7 complements the overview of the above phenomena by displaying the band structure for a long-lattice well-depth $V_\ell = 60\ E_R$. The rich energy structure in the double-well regime ($|V_s| > 30\ E_R$, to the left of the red dotted vertical line) compared to the single-well regime ($|V_s| < 30\ E_R$) is clear in this figure where the closed gaps located at $V_s = -144\ E_R$, $V_s = -(60/7)^2 \approx -73.47\ E_R$, and $V_s = (60/9)^2 \approx -44.44\ E_R$ (i.e., $\kappa = 5, 7, 9$ are indicated by vertical dotted blue lines).

6 Correspondence between orientation/alignment of a planar rotor and spatial localization (squeezing) of an atom in an optical superlattice

The concept of directionality (orientation and alignment) of a planar rotor subject to orienting and aligning combined fields corresponds to the spatial squeezing of atoms in an optical superlattice (see, e.g., Refs. [37, 38]). In order to illustrate this correspondence, we make use of the common measures of orientation and alignment defined, respectively, as the expectation values $\langle \cos\theta \rangle$ and $\langle \cos^2\theta \rangle$. A fully oriented and fully anti-oriented planar rotor is characterized, respectively, by $\langle \cos\theta \rangle = 1$ and $\langle \cos\theta \rangle = -1$. A fully aligned planar rotor satisfies $\langle \cos^2\theta \rangle = 1$ whereas the spatial distribution of the axis of a free planar rotor (when the orienting and aligning interactions are absent) is characterized by the isotropic value $\langle \cos^2\theta \rangle = 1/2$.

Therefore, when the planar rotor is oriented, $\theta \approx 0$, whereas when it is anti-oriented, $\theta \approx \pi$. Similarly, we find alignment when $\theta \approx 0$ or π and anti-alignment for $\theta \approx \pi/2$. Fig. 8 shows a schematic representation of the relationship between orientation and alignment of the rotor and the spatial squeezing of atoms in an optical superlattice with $V_\ell > 0$ and $V_s < 0$. As illustrated in the figure, an oriented planar rotor is equivalent to the case of $\theta_a \approx 0$, i.e., the spatial localization of the atomic wavefunction (probability density) at the local minimum of the lattice. On the contrary, an anti-oriented planar rotor is analogous to the case of spatial localization at the global minimum[1].

Fig. 9 shows the probability densities $|\psi(\theta_a)|^2$ of two different bound states of an atom in an optical superlattice and their analogues in the PR system $|\phi(\theta)|^2$: (a) a highly localized state around the global minimum, and (b) a nearly delocalized state. Panel (a) corresponds to $\langle\cos\theta\rangle = -0.964$ and $\langle\cos^2\theta\rangle = 0.931$, which can be characterized as an anti-oriented and aligned pendular state. Panel (b), on the other hand, corresponds to $\langle\cos\theta\rangle = 0.095$ and $\langle\cos^2\theta\rangle = 0.459$, a characteristic of an almost isotropic state ($\langle\cos\theta\rangle \approx 0$).

As mentioned before, the band-edge state at the closed gaps (i.e., a doubly degenerate state) results from a superposition of two driven rotor's states with different Γ symmetries and hence, different localizations. An example is shown in Fig. 10, where the probability densities $|\phi_1^{(A_2)}(\theta)|^2$ and $|\phi_2^{(A_1)}(\theta)|^2$ corresponding to the lowest closed gap at $\kappa = 1$ are depicted. In this case, orientation and alignment of the state associated with A_2 symmetry (the light blue curve localized around the global minimum of the lattice) are $\langle\cos\theta\rangle = -0.886$ and $\langle\cos^2\theta\rangle = 0.793$, respectively. However, for the A_1 symmetry (the purple curve localized around local minimum of the lattice) we find $\langle\cos\theta\rangle = 0.9603$ and $\langle\cos^2\theta\rangle = 0.925$. Consequently, the superposition will be still (nearly) aligned but does have approximately zero orientation (double-arrow like). Note that the discussion given above also applies to the antiperiodic states.

Based on the correspondence between the PR and OSL systems, we introduce the expectation values $\langle\cos\theta_a\rangle$ and $\langle\cos^2\theta_a\rangle$ as quantitative measures of the spatial localization of the Bloch states in an optical superlattice. This makes it possible to use the Hellmann-Feynman theorem to establish a relationship between the spatial dependence of the band-edge energies, such as those shown in Figs. 5,6,7, and the spatial localization of the corresponding eigenstates [46, 47]. According to the Hellmann-Feynman theorem, $\langle\psi_n\,|\partial_\chi H(\chi)|\,\psi_n\rangle = \partial_\chi E_n$ for χ a parameter in the Hamiltonian, which in our case is either V_ℓ or V_s. Hence we obtain (over a single unit cell and for a constant q),

$$\langle\cos\theta_a\rangle_n = \frac{\partial E_n}{\partial V_\ell} \qquad \left\langle\cos^2\theta_a\right\rangle_n = \frac{\partial E_n}{\partial V_s} \tag{20}$$

Therefore, the Hellmann-Feynman theorem implies that variations of the band energy in the vicinity of the genuine and avoided crossings will result in significant changes in the spatial localization of the atoms (see Ref. [46] for further details in the case of the PR system). From Eq. 20 and given that the global minimum of the potential $V(x)$ rises whereas the local minimum of the potential drops at the avoided crossings (see Sec. 2), the localization of band-edge states around $\theta_a = 0$ and $\theta_a = \pi$ interchanges, although the symmetry of the states involved remains the same.

We note that the abrupt changes in the localization of the wavefunctions at these intersections are characteristic of energy levels well below the maximum of the potential but still above the local minimum. Indeed, for higher excited states, those changes occur more smoothly.

[1] Note that by choosing $V_\ell < 0$, localization around the local/global minimum would be analogous to antiorientation/orientation.

7 Conclusions and prospects

We have shown that two seemingly unrelated systems – an atom under the potential of an optical superlattice and a planar rigid rotor under combined orienting and aligning interactions (also known as the generalized planar pendulum in our previous works) – have isomorphic Hamiltonians. We made use of this isomorphism and applied the extensive results obtained previously for the latter case based in part on the theory of the Whittaker-Hill equation [4, 46] to treat atoms in an optical superlattice. Given that the eigenproblem of a planar rotor in combined fields is conditionally quasi-exactly solvable, we have been able to obtain analytic results for atoms in an optical superlattice as well. These analytical solutions correspond to the edge states of the OSL band structure.

In particular, we have obtained in analytic form a finite number of eigenstates corresponding to the deep-lying band edges around the global minimum of the superlattice potential. Thereby, we prepared the soil for obtaining exact expressions for tunneling amplitudes between the sites of the superlattice (such as two global minima) and hence the hopping term in the corresponding Hubbard model Hamiltonian or the Landau-Zener tunneling probabilities [49]. By invoking the spectral properties of the Whittaker-Hill equation, we have shown that the motion of ultracold atoms in an optical superlattice gives rise to a semifinite-gap system that can be used to study topological properties of the atoms' energy spectra [43, 7, 23]. Finally, we have shown how orientation and alignment of the planar rotor in interacting with external fields translate into the localization (squeezing) of the ultracold atoms in an optical superlattice. This treatment of atom squeezing offers itself to studying transport in optical superlattices [6].

Conversely, the isomorphism between the Hamiltonians of two systems would make it possible to simulate the planar rotor in the presence of external fields by the optical superlattice. In particular, ultracold atoms in an optical superlattice could be used to simulate the semifinite-gap spectrum of the supersymmetric partners of the planar rotor under the orienting and aligning interactions as well as under more involved potentials [39, 58, 57]. Therefore, the present study can be viewed as a proposal for a quantum simulator of a planar rotor subject to external fields.

In future work, the available analytic solutions will be used to develop analytic dynamical models of the trapping of atoms in an optical superlattice. In addition, in the case of non-zero relative phase, the QES condition provided here should be reconsidered and the topological index κ should be redefined. The solvability of this problem is the subject of our forthcoming work.

We note that ultracold atoms in optical lattices are generally studied via the properties of the Mathieu equation that the time-independent Schrödinger equation for a simple 1D optical lattice $\propto \cos^2(kx)$ [76] reduces to. However, as we have shown herein, using the Whittaker-Hill equation instead, with its intriguing spectral features as well as its conditional quasi-exact solvability, reveals new perspectives on the optical superlattice eigenproblem that could prove useful in band structure engineering of ultracold quantum gases. This is a further indication that the fields of ultracold atoms, coherent control, and condensed matter physics are coming closer together.

A Analytically obtainable band-edge states

The eigenstates of the PR Hamiltonian can be obtained in analytic form by diagonalizing the four finite-dimensional symmetry-adapted matrix representations of this Hamiltonian. The solutions that satisfy the $q = 0$ (periodic boundary condition) can be written as

$$
\begin{aligned}
\psi^{(A_1)}(\theta_a) &= \left(N^{(A_1)}\right)^{-1/2} e^{\beta\cos\theta_a} \sum_{\ell=0}^{(\kappa-1)/2} v_\ell \cos^{2\ell}\frac{\theta_a}{2} \\
\psi^{(A_2)}(\theta_a) &= \left(N^{(A_2)}\right)^{-1/2} e^{\beta\cos\theta_a} \sin\theta_a \sum_{\ell=0}^{(\kappa-3)/2} \tilde{v}_\ell \cos^{2\ell}\frac{\theta_a}{2}
\end{aligned}
\tag{21}
$$

which are normalized by (on the 2π interval of θ_a)

$$
\begin{aligned}
N^{(A_1)} &= 2\pi \sum_{\ell,\ell'} \frac{1}{2^{2L}} v_\ell v_{\ell'} \left\{ \binom{2L}{L} I_0(2\beta) + 2\sum_{j=0}^{L-1} \binom{2L}{j} I_{L-j}(2\beta) \right\} \\
N^{(A_2)} &= 2\pi \sum_{\ell,\ell'} \frac{1}{2^{2L+1}} \tilde{v}_\ell \tilde{v}_{\ell'} \left\{ \binom{2L}{L} I_1(2\beta)/\beta + \sum_{j=0}^{L-1} \binom{2L}{j} [2I_{L-j}(2\beta) - I_{L-j+2}(2\beta) \right. \\
&\quad \left. - I_{L-j-2}(2\beta)] \right\}
\end{aligned}
\tag{22}
$$

The constants v_ℓ and $\tilde{v}_\ell$ are components of the eigenvectors of the matrix representations corresponding to the A_1 or A_2 symmetries (see Refs. [4, 46]). I_ρ is the modified Bessel function of the first kind and ρth order [2, 20], $\binom{b}{a}$ is the binomial coefficient, and $L := \ell + \ell'$.

The 2π-antiperiodic solutions can be written as

$$
\begin{aligned}
\psi^{(B_1)}(\theta_a) &= \left(N^{(B_1)}\right)^{-1/2} e^{\beta\cos\theta_a} \cos\frac{\theta_a}{2} \sum_{\ell=0}^{(\kappa-2)/2} w_\ell \cos^{2\ell}\frac{\theta_a}{2}\,, \\
\psi^{(B_2)}(\theta_a) &= \left(N^{(B_2)}\right)^{-1/2} e^{\beta\cos\theta_a} \sin\frac{\theta_a}{2} \sum_{\ell=0}^{(\kappa-2)/2} \tilde{w}_\ell \cos^{2\ell}\frac{\theta_a}{2}
\end{aligned}
\tag{23}
$$

where, the constants w_ℓ and $\tilde{w}_\ell$ are components of the eigenvectors of the matrix representations associated with the B_1 and B_2 symmetries given in Refs. [4, 46]. The normalization constants are

$$
\begin{aligned}
N^{(B_1)} &= 2\pi \sum_{\ell,\ell'} \frac{1}{2^{2L+1}} w_\ell w_{\ell'} \left\{ \binom{2L}{L} [I_0(2\beta) + I_1(2\beta)] + \sum_{j=0}^{L-1} \binom{2L}{j} [2I_{L-j}(2\beta) \right. \\
&\quad \left. + I_{L-j+1}(2\beta) + I_{L-j-1}(2\beta)] \right\} \\
N^{(B_2)} &= 2\pi \sum_{\ell,\ell'} \frac{1}{2^{2L+1}} \tilde{w}_\ell \tilde{w}_{\ell'} \left\{ \binom{2L}{L} [I_0(2\beta) - I_1(2\beta)] + \sum_{j=0}^{L-1} \binom{2L}{j} [2I_{L-j}(2\beta) \right. \\
&\quad \left. - I_{L-j+1}(2\beta) - I_{L-j-1}(2\beta)] \right\}
\end{aligned}
\tag{24}
$$

A total of 40 analytic solutions are given in Refs. [4, 46]. Note that these analytic solutions are limited to the so-called interval of quasi-exact solvability. Above this interval all the solutions are only obtainable by means of the numerical methods. However, those on the loci of integer κ maintain the same expression given by Eqs. 21,23 but with coefficients calculated numerically.

Fig. 11 displays 24 of the analytic energy curves as a functions of β for different values of κ. It is important to keep in mind that the superlattice geometry changes from a single-well for $\beta < \kappa/2$ to a double-well per site for $\beta > \kappa/2$.

B The Hill discriminant

Consider the differential equation

$$\frac{d^2 f}{dy^2} + [\lambda + Q(y)]f(y) = 0 \tag{25}$$

where $Q(y + T) = Q(y)$ is a real-valued smooth periodic function and λ is the eigenvalue. This periodic differential equation (often called the Hill equation [44]) has a band-gap structure. Due to the translational symmetry, functions $f(y)$ should fulfil the following boundary condition

$$f(y + T) = \mu f(y) \tag{26}$$

where μ is known as the Floquet multiplier.

In order to study its spectrum, we choose a basis set consisting of two linearly independent solutions $f_1(y, \lambda)$ and $f_2(y, \lambda)$ corresponding to the same eigenvalue λ and obeying the conditions $f_1(0, \lambda) = f_2'(0, \lambda) = 1$ and $f_2(0, \lambda) = f_1'(0, \lambda) = 0$ (prime denotes the derivative with respect to y). Defining the general f function corresponding to the eigenvalue λ as

$$f(y, \lambda) = \alpha f_1(y, \lambda) + \beta f_2(y, \lambda) \tag{27}$$

and substituting it into Eq. 26 and its derivative, we have

$$\begin{bmatrix} f_1(T, \lambda) & f_2(T, \lambda) \\ f_1'(T, \lambda) & f_2'(T, \lambda) \end{bmatrix} \begin{bmatrix} \alpha \\ \beta \end{bmatrix} = \mu \begin{bmatrix} \alpha \\ \beta \end{bmatrix} \tag{28}$$

The 2-by-2 matrix on the left hand side of Eq. 28 is the transpose of the monodromy matrix with a constant (y-independent) determinant equal to one [69, 7, 44]. It is known that the eigenvalues of the monodromy matrix, μ, are Floquet multipliers and that the trace of the monodromy matrix,

$$\mathcal{D}(\lambda) = f_1(T, \lambda) + f_2'(T, \lambda)\ , \tag{29}$$

is the discriminant associated with the Hill equation (25), the so-called Hill discriminant or Floquet discriminant [7, 23]. Note that some authors define $\mathcal{D}(\lambda)$ as half of this value (see e.g. Refs. [33, 69]). Thus, from Eq. 28, the characteristic equation for the eigenvalues μ reduces to

$$\mu^2 - \mathcal{D}(\lambda)\mu + 1 = 0 \tag{30}$$

By substituting $\mu = \exp(iTq)$ in Eq. 30, we obtain the relation between the Hill discriminant and the q parameter as

$$\mathcal{D}(\lambda) = 2\cos(Tq(\lambda)) \tag{31}$$

Finally, the spectral properties of Eq. 25 can be explained by using the oscillation properties of its associated Hill discriminant $\mathcal{D}(\lambda)$ [34, 33, 44, 7]: (i) for $|\mathcal{D}(\lambda)| \leq 2$, the parameter q is real and so the modulus of μ is equal to one. Therefore, the solutions $f(y)$ are bounded and the corresponding λ values are allowed (bands). (ii) for $|\mathcal{D}(\lambda)| > 2$, the parameter q is not real and so the solutions $f(y)$ do not have a finite norm and thus are not physically admissible. The corresponding λ values are forbidden (gaps). Furthermore, the λ values with $\mathcal{D}(\lambda) = 2$ are the spectral edges corresponding to the periodic solutions ($\mu = 1$), and those with $\mathcal{D}(\lambda) = -2$ to the antiperiodic solutions ($\mu = -1$). Therefore, these values describe the edges of the allowed regions (band-edges).

We note that the oscillations of the discriminant $\mathcal{D}(\lambda)$ as a function of real eigenvalues λ and their intersections with lines $\mathcal{D}(\lambda) = \pm 2$ depend on the shape of the periodic function $Q(y)$ in Eq. 25.

References

[1] H. Ammann, R. Gray, I. Shvarchuck, and N. Christensen. Quantum Delta-Kicked Rotor: Experimental Observation of Decoherence. *Phys. Rev. Lett.*, 80(19):4111–4115, may 1998.

[2] G. Arfken and H. Weber. *Mathematical Methods For Physicists*. Elsevier Science, 6th edition, 2005.

[3] B. A. Ashwell, S. Ramakrishna, and T. Seideman. Strong field coherent control of molecular torsions—Analytical models. *J. Chem. Phys.*, 143:064307, 2015.

[4] S. Becker, M. Mirahmadi, B. Schmidt, K. Schatz, and B. Friedrich. Conditional quasi-exact solvability of the quantum planar pendulum and of its anti-isospectral hyperbolic counterpart. *Eur. Phys. J. D*, 71:149, 2017.

[5] L. Cai and B. Friedrich. Recurring Molecular Alignment Induced by Pulsed Nonresonant Laser Fields. *Coll. Czech Chem. Commun.*, 66:991–1004, 2001.

[6] T. Calarco, U. Dorner, P. S. Julienne, C. J. Williams, and P. Zoller. Quantum computations with atoms in optical lattices: Marker qubits and molecular interactions. *Phys. Rev. A*, 70:012306, 2004.

[7] F. Correa, V. Jakubský, and M. S. Plyushchay. Finite-gap systems, tri-supersymmetry and self-isospectrality. *J. Phys. A*, 41:485303, 2008.

[8] D. Daems, S. Guérin, D. Sugny, and H. R. Jauslin. Efficient and Long-Lived Field-Free Orientation of Molecules by a Single Hybrid Short Pulse. *Phys. Rev. Lett.*, 94:153003, 2005.

[9] I. H. Deutsch and P. Jessen. Quantum Information Processing in Optical Lattices: Cold Atomic Qubits in a Virtual Crystal of Light. *IEEE-LEOS Newsl.*, 2002.

[10] P. Djakov and B. Mityagin. Simple and double eigenvalues of the Hill operator with a two-term potential. *J. Approx. Theory*, 135(1):70–104, July 2005.

[11] R. Dutt, A. Khare, and Y. P. Varshni. New class of conditionally exactly solvable potentials in quantum mechanics. *J. Phys. A. Math. Gen.*, 28:L107–L113, 1995.

[12] O. Dutta, M. Gajda, P. Hauke, M. Lewenstein, D.-S. Lühmann, B. A. Malomed, T. Sowiński, and J. Zakrzewski. Non-standard hubbard models in optical lattices: a review. *Reports on Progress in Physics*, 78(6):066001, may 2015.

[13] T. Esslinger. Fermi-hubbard physics with atoms in an optical lattice. *Annual Review of Condensed Matter Physics*, 1(1):129–152, 2010.

[14] S. Fishman, D. R. Grempel, and R. E. Prange. Chaos, quantum recurrences, and anderson localization. *Phys. Rev. Lett.*, 49:509–512, 1982.

[15] T. Fölling, S. and Trotzky, S. and Cheinet, P. and Feld, M. and Saers, R. and Widera, A. and Müller and I. Bloch. Direct observation of second-order atom tunnelling. *Nature*, 448:1029–1032, 2007.

[16] B. Friedrich and Herschbach. Manipulating Molecules via Combined Static and Laser Fields. *J. Phys. Chem. A*, 103:10280–10288, 1999.

[17] B. Friedrich and D. R. Herschbach. On the possibility of orienting rotationally cooled polar molecules in an electric field. *Z. Phys. D - Atoms, Mol. Clust.*, 18:153–161, 1991.

[18] B. Friedrich, D. P. Pullman, and D. R. Herschbach. Alignment and orientation of rotationally cool molecules. *J. Phys. Chem.*, 95:8118–8129, 1991.

[19] A. Gonzalez-Lopez, N. Kamran, and P. Olver. Real Lie algebras of differential operators and quasi-exactly solvable potentials. *Philos. Trans. R. Soc. London. Ser. A Math. Phys. Eng. Sci.*, 354:1165–1193, 1996.

[20] I. S. Gradshtein and I. M. Ryzhik. *Table of Integrals, Series, and Products*. Elsevier Science, 7th edition edition, 2007.

[21] D. R. Grempel, R. E. Prange, and S. Fishman. Quantum dynamics of a nonintegrable system. *Phys. Rev. A*, 29(4):1639–1647, apr 1984.

[22] C. Hamilton and J. Pérez-Ríos. Classical-quantum localization in one dimensional systems: The kicked rotor. *AIP Advances*, 12(3):035040, 2022.

[23] A. D. Hemery and A. P. Veselov. Whittaker–Hill equation and semifinite-gap Schrödinger operators. *J. Math. Phys.*, 51:072108, 2010.

[24] N. E. Henriksen. Molecular alignment and orientation in short pulse laser fields. *Chem. Phys. Lett.*, 312:196–202, 1999.

[25] D. Herschbach. Calculation of Energy Levels for Internal Torsion and Over-All Rotation. III. *J. Chem. Phys.*, 31:91–108, 1959.

[26] F. M. Izrailev. Simple models of quantum chaos: Spectrum and eigenfunctions. *Phys. Rep.*, 196(5-6):299–392, nov 1990.

[27] G. Junker and P. Roy. Conditionally Exactly Solvable Potentials: A Supersymmetric Construction Method. *Ann. Phys. (N. Y).*, 270:155–177, 1998.

[28] J. Kangara, C. Cheng, S. Pegahan, I. Arakelyan, and J. E. Thomas. Atom Pairing in Optical Superlattices. *Phys. Rev. Lett.*, 120:083203, 2018.

[29] A. Kay and J. K. Pachos. Quantum computation in optical lattices via global laser addressing. *New J. Phys.*, 6:1–16, 2004.

[30] T. Kiljunen, B. Schmidt, and N. Schwentner. Intense-field alignment of molecules confined in octahedral fields. *Phys. Rev. Lett.*, 94:2–5, 2005.

[31] B. G. Klappauf, W. H. Oskay, D. A. Steck, and M. G. Raizen. Observation of Noise and Dissipation Effects on Dynamical Localization. *Phys. Rev. Lett.*, 81(6):1203–1206, aug 1998.

[32] C. P. Koch, M. Lemeshko, and D. Sugny. Quantum control of molecular rotation. *Rev. Mod. Phys.*, 91:35005, 2019.

[33] W. Kohn. Analytic properties of Bloch waves and Wannier functions. *Phys. Rev.*, 115(4):809–821, 1959.

[34] H. Kramers. Das eigenwertproblem im eindimensionalen periodischen kraftfelde. *Physica*, 2(1):483–490, 1935.

[35] L. D. Landau and E. M. Lifshitz. *Quantum mechanics: non-relativistic theory*, volume 3. Pergamon Press, 1991.

[36] P. J. Lee, M. Anderlini, B. L. Brown, J. Sebby-Strabley, W. D. Phillips, and J. V. Porto. Sublattice addressing and spin-dependent motion of atoms in a double-well lattice. *Phys. Rev. Lett.*, 99:1–4, 2007.

[37] M. Leibscher and I. S. Averbukh. Squeezing of atoms in a pulsed optical lattice. *Phys. Rev. A*, 65:053816, 2002.

[38] M. Leibscher and B. Schmidt. Quantum dynamics of a plane pendulum. *Phys. Rev. A*, 80:012510, 2009.

[39] M. Lemeshko, M. Mustafa, S. Kais, and B. Friedrich. Supersymmetry identifies molecular Stark states whose eigenproperties can be obtained analytically. *New J. Phys.*, 13:063036, 2011.

[40] T.-H. Leung, M. N. Schwarz, S.-W. Chang, C. D. Brown, G. Unnikrishnan, and D. Stamper-Kurn. Interaction-enhanced group velocity of bosons in the flat band of an optical kagome lattice. *Phys. Rev. Lett.*, 125:133001, Sep 2020.

[41] X. Li and W. V. Liu. Physics of higher orbital bands in optical lattices: a review. *Reports on Progress in Physics*, 79(11):116401, sep 2016.

[42] A. Liapounoff. Sur une série dans la théorie des équations difféntielles du second ordre á coefficients periodiques, mem. *Acad. Imp. Sci. St. Petersbourg (= Akad. Nauk Zapiski)(8) XIII*, page 113, 1902.

[43] M. Lohse, C. Schweizer, O. Zilberberg, M. Aidelsburger, and I. Bloch. A thouless quantum pump with ultracold bosonic atoms in an optical superlattice. *Nature Physics*, 12(4):350–354, 2016.

[44] W. Magnus and S. Winkler. *Hill's Equation*. Dover Publications, 2004.

[45] C. C. Marston and G. G. Balint-Kurti. The Fourier grid Hamiltonian method for bound state eigenvalues and eigenfunctions. *J. Chem. Phys.*, 91:3571, 1989.

[46] M. Mirahmadi. *Spectra and Dynamics of Driven Linear Quantum Rotors: Symmetry Analysis and Algebraic Methods*. Phd thesis, 2020.

[47] M. Mirahmadi, B. Schmidt, and B. Friedrich. Quantum dynamics of a planar rotor driven by suddenly switched combined aligning and orienting interactions. *New J. Phys.*, 23(6):63040, may 2021.

[48] F. L. Moore, J. C. Robinson, C. F. Bharucha, B. Sundaram, and M. G. Raizen. Atom Optics Realization of the Quantum δ-Kicked Rotor. *Phys. Rev. Lett.*, 75(25):4598–4601, dec 1995.

[49] O. Morsch and M. Oberthaler. Dynamics of bose-einstein condensates in optical lattices. *Rev. Mod. Phys.*, 78:179–215, Feb 2006.

[50] S. M. Parker, M. A. Ratner, and T. Seideman. Coherent control of molecular torsion. *J. Chem. Phys.*, 135:224301, 2011.

[51] S. Peil, J. V. Porto, B. L. Tolra, J. M. Obrecht, B. E. King, M. Subbotin, S. L. Rolston, and W. D. Phillips. Patterned loading of a Bose-Einstein condensate into an optical lattice. *Phys. Rev. A*, 67:051603, 2003.

[52] L. F. Roncaratti and V. Aquilanti. Whittaker-Hill equation, Ince polynomials, and molecular torsional modes. *Int. J. Quantum Chem.*, 110:716–730, 2010.

[53] A. Rouzée, A. Gijsbertsen, O. Ghafur, O. M. Shir, T. Bäck, S. Stolte, and M. J. J. Vrakking. Optimization of laser field-free orientation of a state-selected NO molecular sample. *New J. Phys.*, 11:105040, 2009.

[54] R. Roychoudhury, P. Roy, M. Znojil, and G. Levai. Comprehensive analysis of conditionally exactly solvable models. *J. Math. Phys.*, 42:1996, 2001.

[55] F. Schäfer, T. Fukuhara, S. Sugawa, Y. Takasu, and Y. Takahashi. Tools for quantum simulation with ultracold atoms in optical lattices. *Nature Reviews Physics*, 2(8):411–425, 2020.

[56] K. Schatz, B. Friedrich, S. Becker, and B. Schmidt. Symmetric tops in combined electric fields: Conditional quasisolvability via the quantum Hamilton-Jacobi theory. *Phys. Rev. A*, 97:053417, 2018.

[57] B. Schmidt and B. Friedrich. Supersymmetry and eigensurface topology of the planar quantum pendulum. *Front. Phys.*, 2:022111, 2014.

[58] B. Schmidt and B. Friedrich. Topology of surfaces for molecular Stark energy, alignment, and orientation generated by combined permanent and induced electric dipole interactions. *J. Chem. Phys.*, 140:064317, 2014.

[59] B. Schmidt and C. Hartmann. WavePacket: A Matlab package for numerical quantum dynamics.II: Open quantum systems, optimal control, and model reduction. *Comput. Phys. Commun.*, 228:229–244, 2018.

[60] B. Schmidt, R. Klein, and L. Cancissu Araujo. WavePacket: A Matlab package for numerical quantum dynamics. III. Quantum-classical simulations and surface hopping trajectories. *J. Comput. Chem.*, 40(30):2677–2688, 2019.

[61] B. Schmidt and U. Lorenz. WavePacket: A Matlab package for numerical quantum dynamics. I: Closed quantum systems and discrete variable representations. *Comput. Phys. Commun.*, 213:223–234, 2017.

[62] J. Sebby-Strabley, M. Anderlini, P. S. Jessen, and J. V. Porto. Lattice of double wells for manipulating pairs of cold atoms. *Phys. Rev. A*, 73:033605, 2006.

[63] T. Seideman. Rotational excitation and molecular alignment in intense laser fields. *J. Chem. Phys.*, 103:7887–7896, 1995.

[64] T. Seideman and E. Hamilton. Nonadiabatic Alignment by Intense Pulses. Concepts, Theory, and Directions. *Adv. At. Mol. Opt. Phys.*, 52:289–329, 2005.

[65] G. Semeghini, H. Levine, A. Keesling, S. Ebadi, T. T. Wang, D. Bluvstein, R. Verresen, H. Pichler, M. Kalinowski, R. Samajdar, A. Omran, S. Sachdev, A. Vishwanath, M. Greiner, V. Vuletić, and M. D. Lukin. Probing topological spin liquids on a programmable quantum simulator. *Science*, 374(6572):1242–1247, 2021.

[66] M. A. Shifman and A. V. Turbiner. Quantal problems with partial algebraization of the spectrum. *Commun. Math. Phys.*, 126:347–365, 1989.

[67] H. Stapelfeldt and T. Seideman. Aligning molecules with strong laser pulses. *Rev. Mod. Phys.*, 75(2):543–557, 2003.

[68] D. A. Steck. Quantum and Atom Optics, 2019.

[69] G. Teschl. *Ordinary differential equations and Dynamical Systems*. American Mathematical Society, 2012.

[70] C. Tian and A. Altland. Theory of localization and resonance phenomena in the quantum kicked rotor. *New J. Phys.*, 12:043043, 2010.

[71] A. V. Turbiner. Quantum mechanics: problems intermediate between exactly solvable and completely unsolvable. *J. Exp. Theor. Phys.*, 67:230–236, 1988.

[72] A. V. Turbiner. Quasi-exactly-solvable problems and sl(2) algebra. *Commun. Math. Phys.*, 118:467–474, 1988.

[73] J. von Neumann and E. P. Wigner. Zur Erklärung einiger Eigenschaften der Spektren aus der Quantenmechanik des Drehelektrons. *Phys. Z.*, 30:467–470, 1929.

[74] L. Wang, M. Troyer, and X. Dai. Topological charge pumping in a one-dimensional optical lattice. *Phys. Rev. Lett.*, 111(2):1–5, 2013.

[75] E. T. Whittaker. On a class of Differential Equations whose solutions satisfy Integral Equations. *Proc. Edinburgh Math. Soc.*, (December):14–23, 1914.

[76] P. Windpassinger and K. Sengstock. Engineering novel optical lattices. *Reports Prog. Phys.*, 76:086401, 2013.

[77] S. Winkler and W. Magnus. The coexistence problem for Hill's equation. In *Research report*, number BR-26, page 108, New York, 1958. New York University.

[78] G. Wirth, M. Ölschläger, and A. Hemmerich. Evidence for orbital superfluidity in the P-band of a bipartite optical square lattice. *Nat. Phys.*, 7:147–153, 2011.

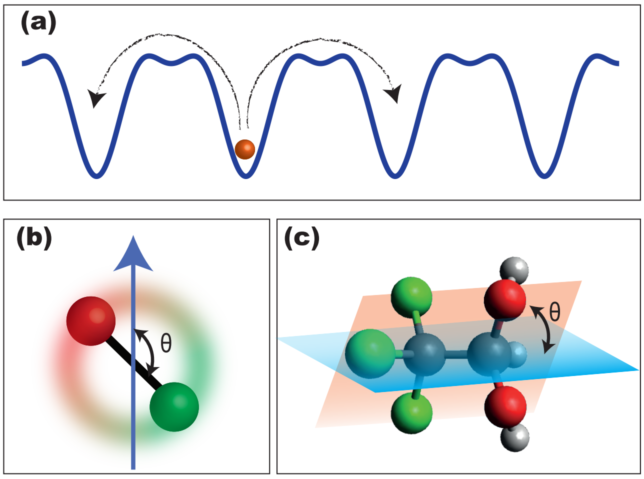

Figure 1: Three different eigenproblems whose Hamiltonians are isomorphic: (a) trapping of ultracold atoms in an optical superlattice; (b) libration of a planar rigid rotor in collinear external electric fields; (c) the torsional motion in a molecule such as $CCl_3CH(OH)_2$.

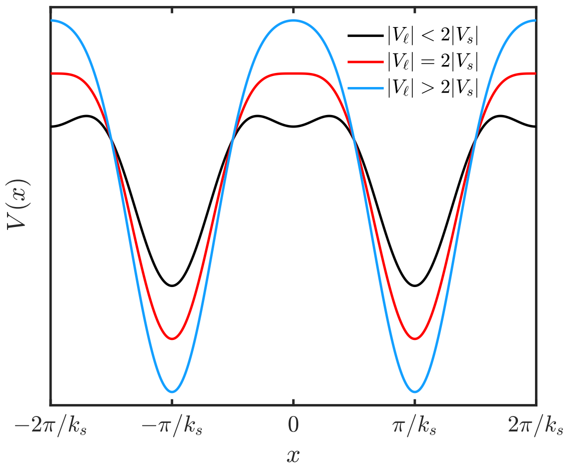

Figure 2: Superlattice optical potential, Eq. 3, for different relative magnitudes of the parameters $V_\ell > 0$ and $V_s < 0$. Note that choosing $V_\ell < 0$ results in a shift in x of $V(x)$ by π/k_s.

DOI 10.20347/WIAS.PREPRINT.2972

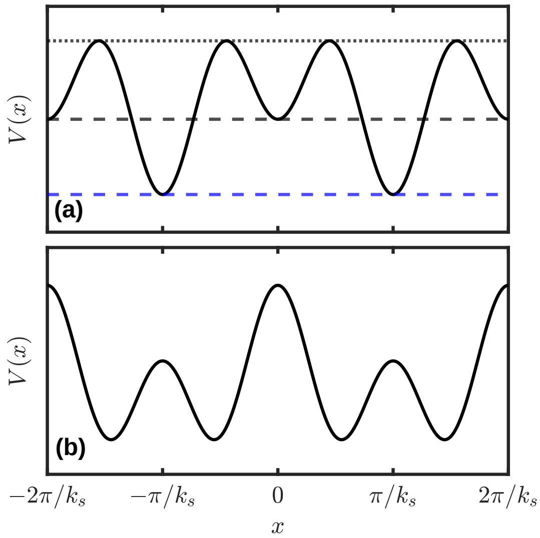

Figure 3: Superlattice optical potential, Eq. 3, for $V_\ell > 0$ and (a) $V_s < 0$ whose local minimum, global minimum, and maximum are marked by the black dashed, blue dashed and black dotted lines, respectively. (b) $V_s > 0$. In either panel, $|V_\ell| < 2\,|V_s|$.

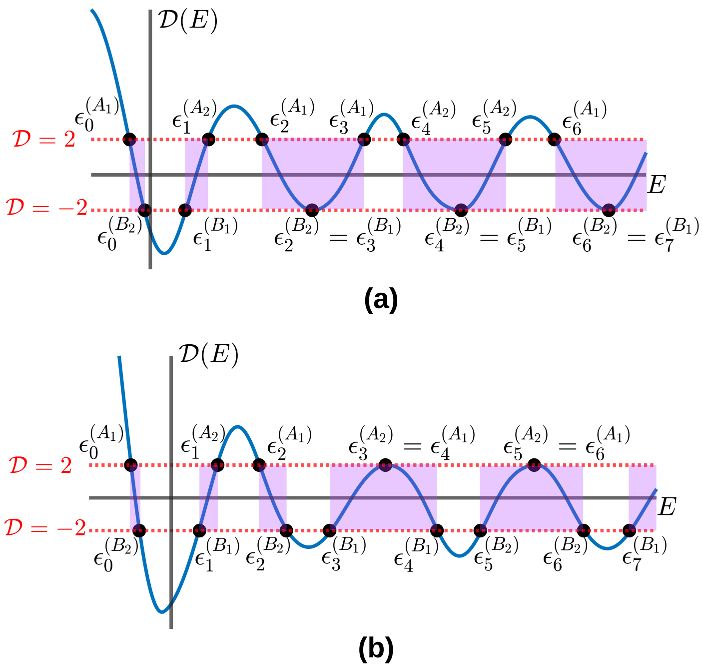

Figure 4: Schematic diagram of the Hill discriminant for atoms in an optical superlattice treated as a semifinite-gap system for (a) $\kappa = 2$ and (b) $\kappa = 3$. The shaded areas indicate the allowed energy (E) regions for $|\mathcal{D}(E)| \leq 2$. Note that the widths of the bands and gaps depend on the choice of the values of the V_s and V_ℓ parameters.

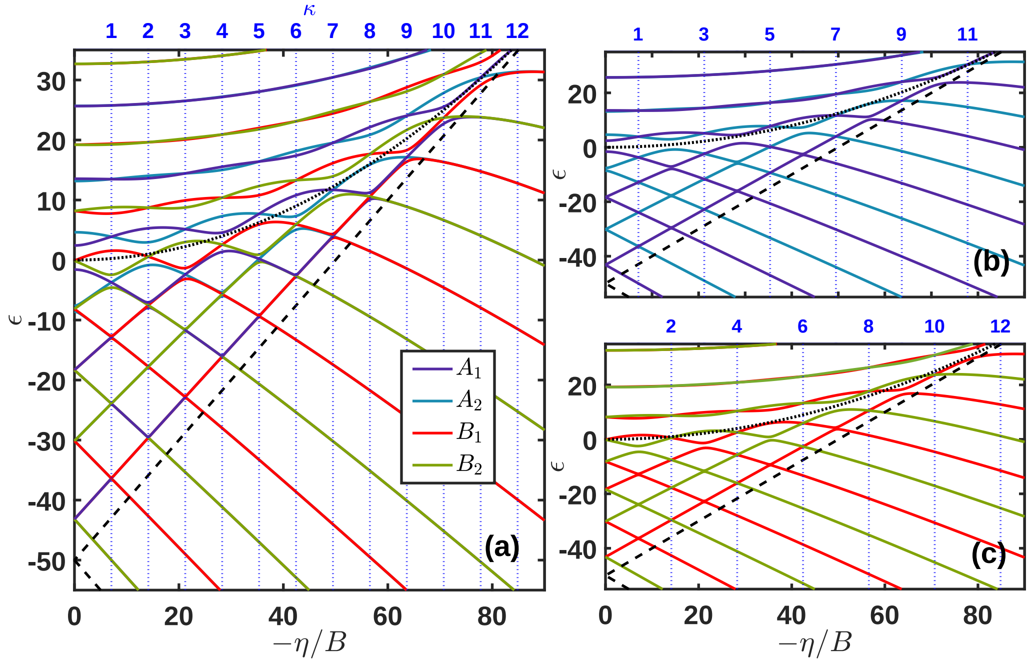

Figure 5: (a) Energies of the planar rotor interacting with combined fields as functions of η for constant $\zeta = 50\ B$. The vertical blue dotted lines mark the η values associated with the integer values of κ from $\kappa = 1$ ($\eta = -\sqrt{50}$) to 14 ($\eta = -14\sqrt{50}$). Panels (b) and (c) show the energies of the periodic (A_1, A_2) and antiperiodic (B_1, B_2) states, respectively. Here, the potential is an asymmetric double well with local and global minima indicated by black dashed lines, and a maximum shown by the black dotted curve.

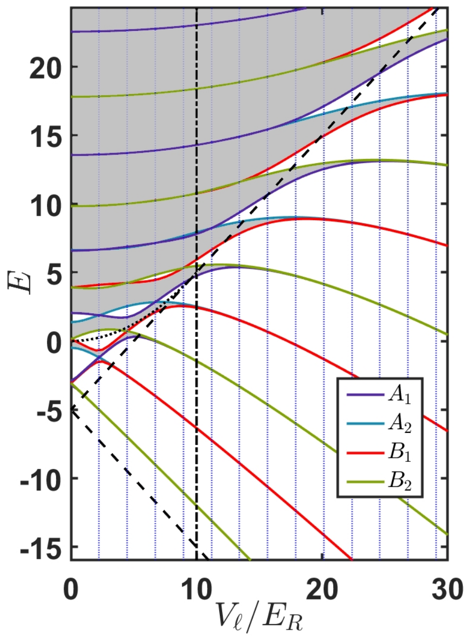

Figure 6: The band-gap structure of the optical superlattice with respect to the long-lattice depth when the short-lattice depth is constant $V_s = -5\ E_R$. The allowed bands are shaded in grey. Blue vertical dotted lines mark V_ℓ corresponding to $\kappa = 1$ to $\kappa = 13$. The black dashed vertical line at $V_\ell = 2|V_s| = 10\ E_R$ distinguishes the double-well (left side) and single-well (right side) regimes. For the single-well regime, black dashed lines indicate the maximum and minimum of the potential. For the double-well regime, see Fig. 5.

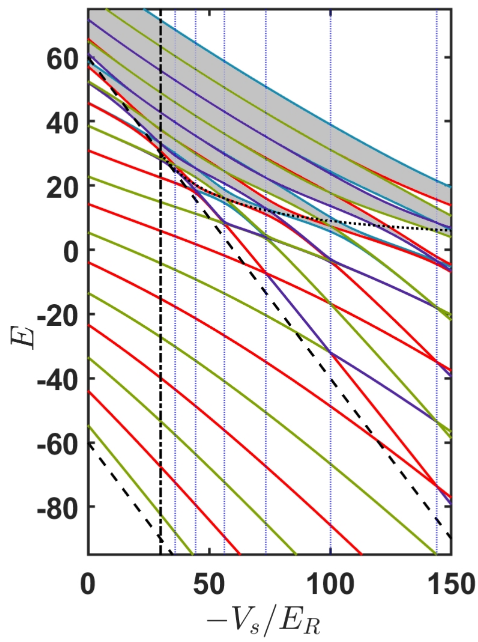

Figure 7: The band-gap structure of atoms in an optical superlattice with respect to the short-lattice depth when the long-lattice depth is constant $V_\ell = 60\ E_R$. Blue dotted lines mark V_s corresponding to κ from $\kappa = 5$ to $\kappa = 10$. The black dashed vertical line at $-V_s = V_\ell/2 = 30\ E_R$ separates the single-well (left side) and double-well (right side) regimes. In the single-well regime, black dashed lines indicate the maximum and minimum of the potential. For the double-well regime, the local and global minima are shown, respectively, by black dashed lines, and the maximum by the black dotted curve, cf. Fig. 5. The color-coding is the same as in Fig. 6.

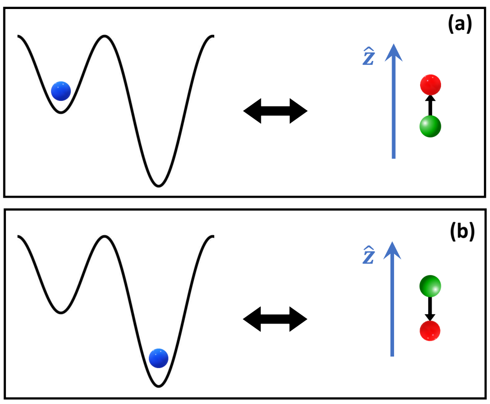

Figure 8: Correspondence between orientation of a planar rotor and spatial localization (squeezing) of an atom in an optical superlattice with $V_\ell > 0$ and $V_s < 0$. Panel (a) shows the oriented rotor ($\theta = 0$) and panel (b) the anti-oriented rotor ($\theta = \pi$). Here, $\hat{z}$ indicates the direction of the collinear external fields.

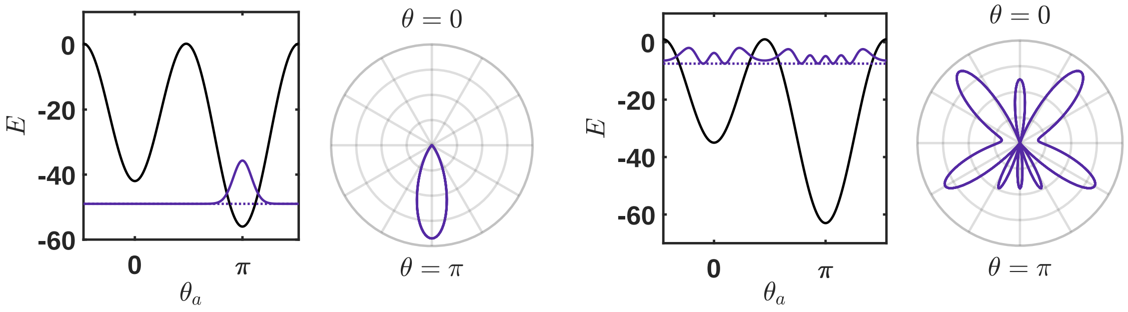

(a) $|\phi_0^{(A_1)}(\theta)|^2$ (ground state) for $\eta = -7\ B$ equivalent to $V_\ell = 7\ E_R$ (i.e., $\kappa = 1$).

(b) $|\phi_6^{(A_1)}(\theta)|^2$ for $\eta = -14\ B$ equivalent to $V_\ell = 14\ E_R$ (i.e., $\kappa = 2$).

Figure 9: Plots of the probability density $|\psi(\theta_a)|^2$ in the unit cell of an optical superlattice for $V_s = -49\ E_R$, together with the polar plots of a planar rotor subject to external fields, $|\phi(\theta)|^2$ with $\zeta = 49\ B$.

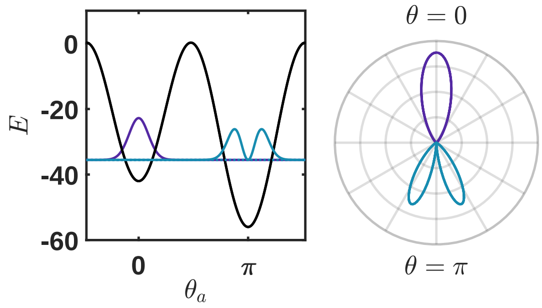

Figure 10: Same as in Fig. 9 but for a genuine crossing at $\zeta = 49\ B$ and $\eta = -7\ B$ or, equivalently, a closed gap at $V_s = -49\ E_R, V_\ell = 7\ E_R$. The color coding is the same as in Fig. 6.

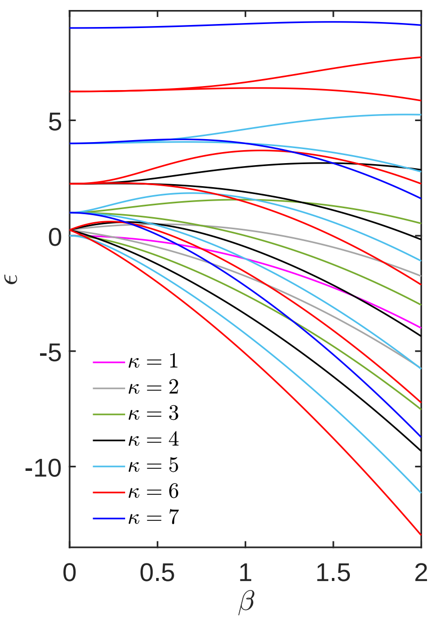

Figure 11: The lowest available analytic eigenvalues of planar rotor in the combined fields (band-edge energies in optical superlattice) as functions of $\beta = \sqrt{\zeta/B} = \sqrt{-V_s/E_R}$ for different integer values of the topological index κ given by Eq. 16.